

Excited states and optical response of a donor–acceptor substituted polyene: A TD-DFT study

Chao Wu ^a, Sergei Tretiak ^{b,*}, Vladimir Y. Chernyak ^a

^a Department of Chemistry, Wayne State University, 5101 Cass Avenue Detroit, MI 48202, United States

^b Theoretical Division, Center for Nonlinear Studies, and Center for Integrated Nanotechnologies, Los Alamos National Laboratory, Mail Stop B268, Los Alamos, NM 87545, United States

Received 26 September 2006; in final form 5 November 2006

Available online 18 November 2006

Abstract

Optical properties of polar push–pull chromophore (diphenylpolyene with donor/acceptor terminal substituents) are studied using hybrid time-dependent density functional theory (TD-DFT). The optical transitions are thoroughly examined. This includes one- and two-photon absorption, and fluorescence, as a function of the underlying density functional, the basis set choice, and the solvent. Calculated excited state properties are found to be strongly dependent on the density functional model used. Hybrid approximations with small fractions of the orbital exchange (e.g. B3LYP) strongly favor zwitterionic-type states with pronounced charge-transfer character. Models with large percentage of orbital exchange (e.g. BHandHLYP) result in neutral-base electronic excitations.

© 2006 Elsevier B.V. All rights reserved.

1. Introduction

During the past years, extraordinary experimental advances have rendered the manipulation and fabrication of structures at the nanoscale possible. Despite parallel developments of theoretical and simulation capabilities, the quantitative understanding and prediction of fundamental macroscopic properties are yet to be achieved. Polarization of a material induced by an external optical field constitutes an example of such an important electronic property. Optical nonlinearities in organic conjugated materials recently received a lot of attention due to their highly polarizable π -electron systems. The nonlinear optical (NLO) response of a large molecular system also strongly depends on the system size and chemical composition [1–4]. Simple substitution with polar donor/acceptor groups can enhance molecular NLO response by orders of magnitude. Materials with large second- and third-order

NLO responses can be utilized for a variety of applications [5,6]. For example, a search for molecular compounds with high two-photon absorption (TPA) efficiency has been pursued since a few years, with the aim to obtain molecules or molecular materials suitable for applications in different fields [7,8], including two-photon laser scanning microscopy, photodynamic therapy, optical power limitation, microfabrication and 3D optical data storage.

Computer design of nonlinear chromophores should allow accurate prediction of stable conformational structures of complex molecules, their fluorescent properties, and nonlinear optical responses and allow the understanding of the underlying structure–property relations, which would ultimately guide organic synthesis. This requires an effective tool for computing the excited state electronic structure and/or the optical response. Although a relatively new field, time-dependent density functional theory (TD-DFT) has rapidly emerged as an extremely useful method for studying the optical response of large molecules [9–11]. Similar to the case of ground-state density functional theory, the number of applications is growing exponentially. For many systems, it yields computational accuracy

* Corresponding author. Fax: +1 505 665 4063.

E-mail addresses: serg@cnls.lanl.gov (S. Tretiak), chernyak@chem.wayne.edu (V.Y. Chernyak).

for the electronic excitation energies within tenths of eV, excited state bond lengths within 1%, dipole moments and vibrational frequencies within 5%, not to mention that the computational cost scales very favorably with the number of electrons. Recently we have suggested an extension of the TD-DFT for calculations of the frequency dependent NLO optical response [12]. This uses a quasiparticle representation of the equation of motion for the density matrix driven by an external field followed by a perturbative expansion in the driving field. TD-DFT has shown a better agreement with experiments than both semiempirical and low level *ab initio* calculations for TPA calculations in large quadrupolar conjugated organic chromophores [4,13,14] and small molecules [15].

In spite of this success, one of the greatest challenges towards the universal applicability of TD-DFT remains the inability of popular density functionals (and their kernels) to routinely and accurately describe certain excitations with a long-range spatial extent [16–19]. For example, charge transfer (CT) states correspond to excitations with weak overlap of the photo-excited electron and hole wavefunctions. This problem is complicated by ignoring an important derivative discontinuity in most functionals. This results in a mismatch of ionization potentials between the donor and acceptor portions of a molecule [20]: TD-DFT tends to underestimate the excitation energies of charge-transfer states, and as a result often places the latter below optical states.

In this Letter, we address this issue and explore the TD-DFT performance by simulating the excited state properties and optical response of ‘push–pull’ donor–acceptor substituted conjugated polyene shown in Fig. 1. A julolidine donor and a nitrophenyl acceptor are highly polar substituents, which leads to strong intramolecular charge transfer. The molecule denoted as 3|5| in the previous studies has been investigated experimentally including absorption, resonance Raman and hyper-Raman studies, second and third harmonic generation [3,21,22]. These studies point to several electronic excited states that dominate the observed spectra. Here we explore the low-lying excited electronic states using different hybrid density functional approaches and analyze the emerging trends. Overall, it is hard to suggest an ideal DFT model for such polar chromophores. Yet, hybrid DFT methods with high content

of the orbital exchange (e.g. BHandHLYP) reproduce physically reliable results that are pretty consistent with experimental data.

The manuscript is organized as follows. Details of our numerical modeling are presented in Section 2. In Section 3 we analyze computational results obtained via different DFT approximations. Finally, in Section 4 we discuss the emerging trends and summarize our findings.

2. Computational methodology

Ground state geometry optimizations for the charge-neutral 3|5| chromophore (Fig. 1) have been performed using Turbomole program suite [23]. The lowest excited state geometries are obtained next using Turbomole as well. This code is capable of searching for a minimum of the TD-DFT excitation energy surface with respect to nuclear coordinates by using analytical gradient techniques [24]. All optimizations are performed in gas phase by using the SV basis set and selected density functionals (see below). The SV and similar 6-31G basis sets are known to be an efficient blend of accuracy and manageable size for large conjugated molecules [13]. For geometry optimization, three common density functionals have been pre-selected that have various fractions of orbital exchange, namely Hartree–Fock (HF) (100%), BHandHLYP (50%), and B3LYP (20%). This set of density functionals represents a gradual decreasing fraction of exchange. In our calculations we never use purely local (Local density approximation, LDA) as well as semi-local (Generalized gradient approximation, GGA) models, which fail to properly describe the underlying long-range interactions that stand behind the charge-transfer phenomena. These models are not just quantitatively inaccurate, but are also qualitatively wrong.

Based on the optimized geometries, we calculate the corresponding TD-DFT excited state structures up to 20 lowest excited states using the GAUSSIAN 98 package [25] to obtain the absorption and fluorescence electronic spectra. Here we use another set of three functionals, BHandHLYP (50%), PBE1PBE (25%), and B3LYP (20%), in combination with the 6-31G basis set. Compared to geometry optimization, we replace the HF, which tends to severely overestimate the excitation energies with a quantitatively more accurate PBE1PBE model. The solvent effects are analyzed by using the polarizable continuum model (PCM), which is based on the integral equation formalism (IEF) [26–29] as implemented in GAUSSIAN 98 [25]. Electronic structures have been calculated for selected compounds in the presence of acetone since this solvent has been also used in experimental studies. To infer the basis set size effects we then vary the basis sets (3-21G, 6-31G, 6-31G(d,p), and 6-31+G(d,p)) upon a fixed BHandHLYP approximation for both geometry optimizations and electronic excitation calculations.

The trends in our computational results are interpreted using a natural transition orbital (NTO) analysis. This

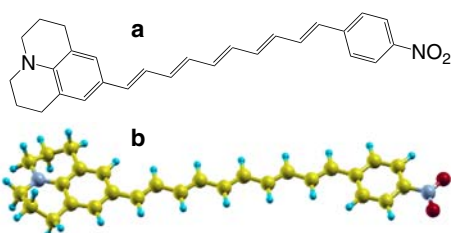


Fig. 1. The push–pull 3|5| chromophore studied: (a) chemical diagram; (b) optimal ground state geometry obtained with BHandHLYP/SV technique. The TPA energies are rescaled ($\times 2$) to superimpose positions of OPA and TPA peaks.

allows to identify and visualize the electronic excitations in question [30]. The transition orbitals provide a graphical real-space representation of the transition densities associated with the molecular electronic excitations computed within the TD-DFT. This analysis offers the most compact description of a given transition density in terms of its expansion via single-particle Kohn–Sham (KS) transitions. The Gaussian code was locally modified to enable performing the NTO analysis.

Finally, we apply the obtained results for the electronic structure by utilizing the approach described in [12,13] to model one- and two-photon absorption spectra. The one-photon absorption (OPA) cross-section at frequency ω is determined by the imaginary part of the polarizability [31]

$$\alpha(\omega) = \sum_v \frac{f_{gv}}{\Omega_{gv}^2 - (\omega + i\Gamma)^2}. \quad (1)$$

Here Ω_{gv} , Γ , and f_{gv} are, respectively, the vertical transition frequency, the empirical linewidth, and the oscillator strength associated with the transition from $|g\rangle$ to $|v\rangle$ electronic state. Similarly the TPA cross-section at frequency ω is determined by the imaginary part of the third order polarizability γ

$$\sigma_{TPA}(\omega) = \frac{4\pi^2\hbar\omega^2}{n^2c^2} L^4 \text{Im}\langle\gamma\rangle, \quad (2)$$

where \hbar , c , n , L , and $\langle\gamma\rangle$ are, respectively, the Planck's constant, the speed of light, the medium refractive index, the local-field factor, and the spatial average of $\gamma(\omega, \omega, -\omega)$, which is calculated by using density matrix formalism [12,13].

3. Results and discussion

3.1. Molecular geometries

For all methods used, planar optimal geometries have been obtained, for both ground state and the first excited state (see Fig. 1b), except for the sterically distorted julolidine end. However, we do see subtle differences in C–C bond lengths along the bridge which strongly affect the excited states electronic properties. The bond-length alternation (BLA) parameter, defined as the difference between C–C and C=C bond lengths, characterizes the delocalization degree of π -electrons along the molecule. Small values of BLA correspond to a fully delocalized electronic system, whereas large values of BLA indicate high degree of π -bond Peierls dimerization. Table 1 shows the details of the optimal geometries obtained using different methods. In the ground state, the BLA parameter steadily decreases with decrease of the orbital exchange fraction in the functional. This reflects expected strong electronic localization at HF level and pronounced delocalization when we approach the LDA limit. An opposite trend has been observed for excited state geometry. For the methods with large hybrid content (HF and BHandBLYP) the excited

Table 1

Parameters of the ground state (GS) and the first excited state (ES) optimized molecular geometries of 3|5 chromophore calculated at various theory levels

Method	$\langle C-C \rangle$	$\langle C=C \rangle$	$\langle \text{BLA} \rangle$	Max (BLA)
<i>GS geometry</i>				
HF/SV	1.462	1.346	0.116	0.126
BHandHLYP/SV	1.444	1.356	0.088	0.105
B3LYP/SV	1.444	1.376	0.068	0.087
<i>ES geometry</i>				
HF/SV	1.415	1.391	0.024	0.053
BHandHLYP/SV	1.417	1.384	0.033	0.056
B3LYP/SV	1.453	1.370	0.083	0.117

Bond-length alternation (BLA) parameter refers to the difference between single (C–C) and double (C=C) carbon bonds (Å). Averaging has been done over the π -conjugated bridge bonds between donor and acceptor groups.

state BLA parameter decreases compared to the ground state. This reflects stronger delocalization and long-range π -electron density re-distribution upon photoexcitation. This frequently leads to large optical Stokes shift in the spectra [4]. In contrast, the functional B3LYP with the smallest fraction of the orbital exchange, provides the excited state geometry with the increased BLA parameter. This already suggests that the excited state has localized ionic nature manifesting the charge-transfer problem which may plague such functionals [32]. Finally, we see that the SV and 6-31G basis sets result in almost equivalent optimal structures (not shown). The 6-31G basis set produces slightly larger (by ~ 0.002 Å) BLA compared to its counterpart that results from SV calculations.

3.2. Excited state structure and spectra

The main computational results of the Letter, are presented in Table 2. We tabulated up to four electronic states (including one high-frequency transition) calculated at the ground state geometry. These are naturally relevant for the absorption spectroscopy. Only the lowest-energy state calculated at the excited state geometry is typically contributing to the fluorescence (Kasha's rule). We have also retained the second state in order to illustrate the oscillator strength re-distribution of upon photoinduced vibrational relaxation (see Table 2). Apart from the transition frequency, the oscillator strength unambiguously characterizes the linear absorption. Calculated two-photon absorption cross-section depends on the empirical line-broadening parameter Γ . The computed TPA spectra have large peaks at linear absorption resonances. This makes impossible to determine cross-sections of high-frequency transitions. We used in our calculations a smaller $\Gamma = 0.025$ eV to signify the TPA peaks, compared to its typical value of $\Gamma = 0.1$ eV seen in experiments. Examples of calculated OPA and TPA spectra with the broader line-width $\Gamma = 0.1$ eV are shown in Fig. 2.

Table 2

Excited state structure of the [3]5 chromophore obtained at various theory levels

Method	#	Ω_{GS}	f	σ	#	Ω_{ES}	f	Stokes shift
<i>HF/SV geometry (vacuo)</i>								
BHandHLYP	1	2.86	2.59	2526	1	2.26	3.44	0.60
	2	3.76	0.79	7438	2	3.34	0.35	—
	3	3.83	0.16	4377	—	—	—	—
	7	4.71	0.08	13032	—	—	—	—
PBE1PBE	1	2.13	1.17	6690	1	1.98	2.74	0.15
	2	2.94	1.77	3269	2	2.71	0.95	—
	3	3.06	0.001	521	—	—	—	—
	5	3.74	0.51	3207	—	—	—	—
B3LYP	1	1.97	0.96	7244	1	1.92	2.50	0.05
	2	2.78	1.77	2962	2	2.56	1.12	—
	3	2.88	0.01	368	—	—	—	—
	4	3.54	0.61	—	—	—	—	—
<i>HF/SV geometry (acetone)</i>								
BHandHLYP	1	2.72	2.20	3565	1	1.93	3.45	0.79
	2	3.55	1.27	6440	2	3.02	0.39	—
	3	3.66	0.004	766	—	—	—	—
	6	4.55	0.21	17365	—	—	—	—
PBE1PBE	1	1.87	0.85	8202	1	1.63	2.82	0.24
	2	2.71	1.64	2907	2	2.42	0.93	—
	3	2.87	0.21	—	—	—	—	—
	4	3.62	0.71	—	—	—	—	—
B3LYP	1	1.68	0.70	8884	1	1.57	2.62	0.11
	2	2.54	1.42	2893	2	2.28	1.04	—
	3	2.70	0.36	127	—	—	—	—
	4	3.42	0.75	—	—	—	—	—
<i>BHandHLYP/SV geometry (vacuo)</i>								
BHandHLYP	1	2.66	2.77	2931	1	2.27	3.29	0.39
	2	3.60	0.70	11409	2	3.31	0.47	—
	3	3.71	0.17	9118	—	—	—	—
	7	4.57	0.08	16608	—	—	—	—
PBE1PBE	1	2.05	1.46	7948	1	1.95	2.44	0.10
	2	2.85	1.72	8443	2	2.69	1.22	—
	3	2.98	0.001	1259	—	—	—	—
	5	3.62	0.34	—	—	—	—	—
B3LYP	1	1.91	1.23	8562	1	1.87	2.19	0.04
	2	2.70	1.79	6528	2	2.55	1.40	—
	3	2.82	0.01	791	—	—	—	—
	4	3.42	0.42	—	—	—	—	—
<i>BHandHLYP/SV geometry (acetone)</i>								
BHandHLYP	1	2.50	2.37	4537	1	1.92	3.25	0.58
	2	3.38	1.21	12374	2	2.97	0.60	—
	3	3.51	0.005	2830	—	—	—	—
	6	4.40	0.16	28694	—	—	—	—
PBE1PBE	1	1.78	1.10	10669	1	1.58	2.52	0.20
	2	2.61	1.66	9002	2	2.37	1.14	—
	3	2.78	0.20	110	—	—	—	—
	4	3.49	0.57	—	—	—	—	—
B3LYP	1	1.62	0.92	11359	1	1.51	2.32	0.11
	2	2.45	1.52	7209	2	2.23	1.22	—
	3	2.63	0.33	121	—	—	—	—
	4	3.31	0.63	—	—	—	—	—
<i>B3LYP/SV geometry (vacuo)</i>								
BHandHLYP	1	2.47	2.91	3340	1	2.44	2.45	0.03
	2	3.42	0.65	18762	2	3.28	1.06	—
	3	3.56	0.14	16887	—	—	—	—

Table 2 (continued)

Method	#	Ω_{GS}	f	σ	#	Ω_{ES}	f	Stokes shift
PBE1PBE	1	1.96	1.71	8834	1	1.82	1.22	0.14
	2	2.73	1.65	12438	2	2.64	1.90	—
	3	2.88	0.002	2554	—	—	—	—
B3LYP	1	1.84	1.46	9555	1	1.69	1.04	0.15
	2	2.59	1.77	9710	2	2.51	1.84	—
	3	2.72	0.006	1646	—	—	—	—
	4	3.27	0.28	—	—	—	—	—
<i>B3LYP/SV geometry (acetone)</i>								
BHandHLYP	1	2.31	2.53	5394	1	2.08	2.16	0.23
	2	3.21	1.12	21030	2	2.98	1.52	—
	3	3.36	0.01	16875	—	—	—	—
	6	4.21	0.11	—	—	—	—	—
PBE1PBE	1	1.70	1.33	12472	1	1.42	1.23	0.28
	2	2.49	1.64	14232	2	2.28	1.37	—
	3	2.68	0.19	—	—	—	—	—
	4	3.34	0.43	—	—	—	—	—
B3LYP	1	1.58	1.14	13348	1	1.29	1.12	0.29
	2	2.35	1.57	11688	2	2.13	1.24	—
	3	2.55	0.31	—	—	—	—	—
	4	3.16	0.48	—	—	—	—	—

Calculated are excitation energy Ω (eV), oscillator strength f , TPA cross-section σ (GM) obtained using linewidth of $\Gamma = 0.025$ eV, and Stokes shift (eV). # refers to the state number. Experimentally estimated [21] one-photon energies (oscillator strengths) of three excited states dominating linear absorption spectrum are 2.38 eV (1.58), 2.95 eV (0.66), and 3.37 eV (0.56).

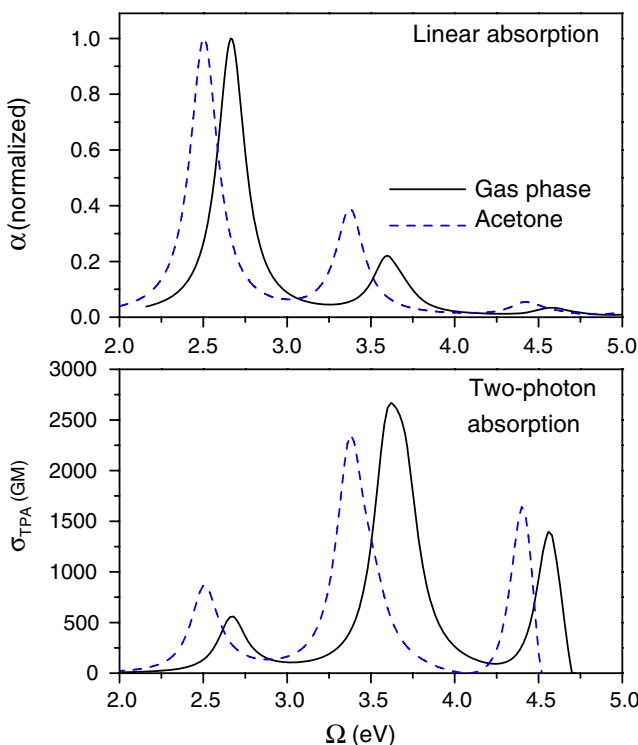


Fig. 2. Calculated OPA (top) and TPA spectra of 3|5| chromophore using TD-BHandHLYP/6-31G//BHandHLYP/SV technique. An empirical damping factor $\Gamma = 0.1$ eV is used to simulate the finite linewidths in the resonant spectra. The spectra in solution (acetone) are modeled using polarizable continuum model [29].

Overall, all the methods used produce three significant electronic states that contribute to different degrees to both linear and two-photon absorption spectra (see Fig. 2). The

three-state effective model previously used for the 3|5| chromophore seems to reasonably describe a variety of spectroscopic data [21]. All these states are of $\pi-\pi^*$ nature and have a pronounced charge-transfer character as illustrated by the natural transition orbitals derived from BHandHLYP and B3LYP results and displayed in Fig. 3. Electron and hole natural orbitals of the lowest state S_1 show a pronounced electronic density shift from the donor to the acceptor groups at both absorption and fluorescence geometries. Compared to S_1 , the higher-energy excited states S_2 (S_3) have more delocalized electron and hole orbitals with nodes in the middle. We also observe a much stronger charge-transfer character in B3LYP orbitals compared to their BHandHLYP counterparts.

Geometries optimized using the HF/SV approach result in the most blue-shifted spectra (Table 2). As expected, the calculated excitation energies shift to the red when undergoing from BHandHLYP to B3LYP limits. The BHandHLYP approximation assigns the largest oscillator strength f to the lowest-energy state S_1 . The relative intensities of the three states in question are consistent with the effective model used to simulate the experimental spectra [21]. In contrast, the second excitation has the largest f for the functionals with the lower fraction of orbital exchange (PBE1PBE and B3LYP). This picture is inverted in the case of TPA spectra, where the second (first) state dominates the results for BHandHLYP (PBE1PBE and B3LYP). We also find a higher lying strong TPA state for BHandHLYP calculations. Excited state relaxation leads to the reduced BLA and red-shifted fluorescence peak frequency. Large Stokes shift of 0.6 eV for the BHandHLYP approach almost vanishes for the B3LYP

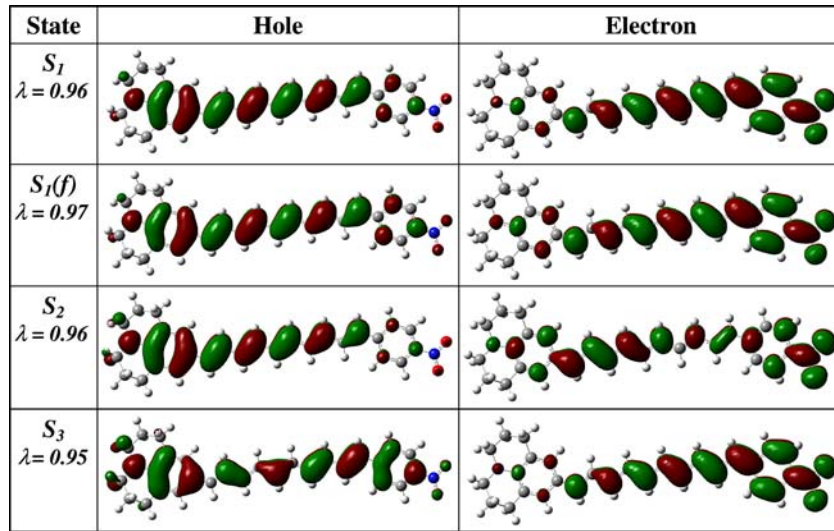


Fig. 3. Natural transition orbitals of several lowest excited states calculated at TD-BHandHLYP/6-31G//BHandHLYP/SV (absorption) and TD-BHandHLYP/6-31G//TD-BHandHLYP/SV (fluorescence) theory level. Parameter λ refers to a fraction of the NTO pair contribution to a given electronic excitation.

method. This emphasizes a substantial difference in the excited state optimal geometries for HF and B3LYP (see Table 1). We also observe an increase in the oscillator strength of the emitting state compared to its absorbing counterpart when using the B3LYP method. The solvation effects are evident: all spectra are red-shifted compared to the isolated molecule results. The Stokes shifts in acetone are larger by about 0.1–0.2 eV compared to the gas phase. This reflects a more polar nature of the emitting state compared to the ground state.

Very similar trends have been observed for the BHandB-LYP/SV optimized geometries. All spectra are red-shifted, and the Stokes shifts become smaller. Oscillator strengths and TPA cross-sections increase, since the reduced BLA parameter favor π -delocalization. Overall, the BHandB-LYP calculations (see Fig. 2) are the most consistent with experimental data [21]. Given the uncertainty of very broad measured spectra, an effective three electronic level model was developed in [21] to simulate absorption spectrum and resonance Raman, hyper-Rayleigh, and hyper-Raman spectra. Some parameters used in this model (excitation energies and oscillator strengths) are given in the caption

of Table 2. Calculated at BHandBLYP level, excited state vibrational reorganization energy on 0.17 eV leading to 0.6 eV Stokes shift in acetone compares well with an experimental fit of solvent reorganization energy (0.11 eV) [21]. For B3LYP optimized geometries, the computed excitation energies are further shifted towards the red. The observed Stokes shifts are small and vanish in the case of BHandBLYP approach. In contrast to HF and BHandBLYP geometries, the oscillator strength in the excited state is reduced. This indicates, that for B3LYP, the optimized excited state geometry converges to the zwitterionic state.

Finally, Table 3 illustrates the basis set size effects. For all techniques, the 6-31G basis set results in the smallest average BLA parameter calculated for the ground state optimal geometries. The BLA tends to slightly increase when the basis set is expanded using the polarized and diffuse functions. As expected, the calculated excitation energies follow the BLA trend: they are blue-shifted for larger BLA parameters. Typically, for fixed geometry, addition of polarized and diffuse functions results in red-shifted excited state frequencies due to the added delocalization space (not shown).

Table 3

Basis set effect on calculated excitation energy Ω (eV), oscillator strength f , and TPA cross-section σ (GM) obtained using linewidth of $\Gamma = 0.025$ eV

3-21 G				6-31G				6-31G(d,p)				6-31+G(d,p)			
$\langle \text{BLA} \rangle = 0.098$				$\langle \text{BLA} \rangle = 0.090$				$\langle \text{BLA} \rangle = 0.093$				$\langle \text{BLA} \rangle = 0.095$			
#	Ω	f	σ												
1	2.79	2.80	2590	1	2.66	2.77	2931	1	2.80	3.01	1823	1	2.85	3.01	1918
3	3.75	0.64	10329	2	3.60	0.70	11409	2	3.83	0.21	14259	2	3.92	0.35	22005
4	3.85	0.22	7886	3	3.71	0.17	9118	3	3.87	0.40	23962	3	3.93	0.33	18269
7	4.73	0.09	12575	7	4.57	0.08	16608	6	4.77	0.04	7638	7	4.87	0.02	11602

Refers to the state number. BHandHLYP functional was used for all computations.

4. Conclusions

In this study we investigate in detail the excited state electronic structure and optical spectra of **3|5|** chromophore using a variety of TD-DFT based techniques. A number of density functionals with varying hybrid content is currently built in the standard electronic structure codes. The choice of an appropriate DFT-based model chemistry for excited state electronic structure simulations of large π -conjugated chromophores is not always obvious. Our results clearly show that a fraction of the orbital exchange, rather than a choice of a specific exchange-correlation GGA model, has drastic effect on the calculated optical properties. In general, the more hybrid component the functional contains, the more localized the π -electronic system tends to be. The ground and lowest-energy excited electronic states of substituted push–pull molecules are often described as a combination of neutral and zwitterionic basis states represented by the corresponding molecular resonance forms [33,34]. The zwitterionic state assumes full separation of positive and negative charges, and, consequently, is optically forbidden. The ‘workhorses’ of quantum chemistry such as B3LYP approximation with only 20% of an orbital exchange may overestimate charge-transfer phenomena, emphasizing zwitterionic-like structures in dipolar molecules substituted with strong donor and acceptor groups, such as **3|5|** chromophore. The ‘neutral-base’ component is underestimated, yet it becomes dominant when the hybrid fraction is increased. These charge-transfer problems become even more severe for the excited state geometry optimizations. Our results show that the functionals with 50% (BHandHLYP) and 20% (B3LYP) shift the optimal geometry in the opposite directions. This has dramatic effects on the excitation energies and peak intensities in the computed spectra. We hope that illustrated performance of hybrid TD-DFT will encourage a cautious approach to DFT-based modeling of polar compounds and will motivate future work on development of new functionals which can better describe delocalized excited states with charge-transfer component.

Acknowledgements

We thank Prof. A. Myers Kelley (UC Merced) for useful discussions. V.Y.C acknowledges the support through the start-up funds from WSU. The research at LANL was carried out under the auspices of the National Nuclear Security Administration of the US Department of Energy. We acknowledge support of Center for Integrated Nanotech-

nology (CINT), Center for Nonlinear Studies (CNLS), and the BES program.

References

- [1] T.G. Goodson, *Acct. Chem. Res.* 38 (2005) 99.
- [2] T.G. Goodson, *Ann. Rev. Phys. Chem.* 56 (2005) 581.
- [3] V. Alain et al., *Adv. Mater.* 11 (1999) 1210.
- [4] C. Katan et al., *J. Phys. Chem. A* 109 (2005) 3024.
- [5] P.N. Prasad, *Introduction to Biophotonics*, Wiley Interscience, New York, 2003.
- [6] P.N. Prasad, *Nanophotonics*, Wiley Interscience, New York, 2004.
- [7] J.D. Bhawalkar, G.S. He, P.N. Prasad, *Rep. Prog. Phys.* 59 (1996) 1041.
- [8] T.C. Lin et al., *Polym. Photon. Appl. II* 161 (2003) 157.
- [9] E.K.U. Gross, J.F. Dobson, M. Petersilka, in: R.F. Nalewajski (Ed.), *Density Functional Theory*, Vol. 181, Springer, Berlin, 1996.
- [10] W. Koch, M.C. Holthausen, *A Chemist’s Guide to Density Functional Theory*, Wiley-VCH, Weinheim, 2000.
- [11] M.E. Casida, in: D.A. Chong (Ed.), *Recent Advances in Density-Functional Methods of Part I*, Vol. 3, World Scientific, Singapore, 1995.
- [12] S. Tretiak, V. Chernyak, *J. Chem. Phys.* 119 (2003) 8809.
- [13] A.M. Masunov, S. Tretiak, *J. Phys. Chem. B* 108 (2004) 899.
- [14] G.P. Bartholomew, M. Rumi, S.J.K. Pond, J.W. Perry, S. Tretiak, G.C. Bazan, *J. Am. Chem. Soc.* 126 (2004) 11529.
- [15] P. Salek, O. Vahtras, J.D. Guo, Y. Luo, T. Helgaker, H. Agren, *Chem. Phys. Lett.* 374 (2003) 446.
- [16] S. Grimme, M. Parac, *Chem. Phys. Chem.* 4 (2003) 292.
- [17] A. Pogantsch, G. Heimel, E. Zojer, *J. Chem. Phys.* 117 (2002) 5921.
- [18] A. Dreuw, J.L. Weisman, M. Head-Gordon, *J. Chem. Phys.* 119 (2003) 2943.
- [19] A. Dreuw, M. Head-Gordon, *J. Am. Chem. Soc.* 126 (2004) 4007.
- [20] D.J. Tozer, *J. Chem. Phys.* 119 (2003) 12697.
- [21] L.C.T. Shoute, M. Blanchard-Desce, A.M. Kelley, *J. Phys. Chem. A* 109 (2005) 10503.
- [22] A.M. Kelley, W.N. Leng, M. Blanchard-Desce, *J. Am. Chem. Soc.* 125 (2003) 10520.
- [23] R. Ahlrichs, M. Bar, M. Haser, H. Horn, C. Kolmel, *Chem. Phys. Lett.* 162 (1989) 165.
- [24] F. Furche, R. Ahlrichs, *J. Chem. Phys.* 117 (2002) 7433.
- [25] M.J. Frisch et al., *GAUSSIAN 98* (Revision A.11), Gaussian Inc., Pittsburgh, PA, 2002.
- [26] E. Cancès, B. Mennucci, J. Tomasi, *J. Chem. Phys.* 107 (1997) 3032.
- [27] M. Cossi, V. Barone, B. Mennucci, J. Tomasi, *Chem. Phys. Lett.* 286 (1998) 253.
- [28] B. Mennucci, R. Cammi, J. Tomasi, *J. Chem. Phys.* 109 (1998) 2798.
- [29] M. Cossi, V. Barone, *J. Chem. Phys.* 115 (2001) 4708.
- [30] R.L. Martin, *J. Chem. Phys.* 118 (2003) 4775.
- [31] S. Mukamel, *Principles of Nonlinear Optical Spectroscopy*, Oxford, New York, 1995.
- [32] R.J. Magyar, S. Tretiak, in press.
- [33] D.Q. Lu, G.H. Chen, J.W. Perry, W.A. Goddard, *J. Am. Chem. Soc.* 116 (1994) 10679.
- [34] A.M. Moran, A.M. Kelley, S. Tretiak, *Chem. Phys. Lett.* 367 (2003) 293.